Spin-density-wave anomaly at 140 K in the ternary iron arsenide BaFe$_2$As$_2$

Marianne Rotter, Marcus Tegel, and Dirk Johrendt[*]

*Department Chemie und Biochemie, Ludwig-Maximilians-Universität München, Butenandtstrasse 5-13, Haus D,
München 81377, Germany*

Inga Schellenberg, Wilfried Hermes, and Rainer Pöttgen

Institut für Anorganische und Analytische Chemie, Universität Münster, Corrensstrasse 30, Münster 48149, Germany

(Received 26 May 2008; published 8 July 2008)

The ternary iron arsenide BaFe$_2$As$_2$, with the tetragonal ThCr$_2$Si$_2$-type structure, exhibits a spin-density-wave (SDW) anomaly at 140 K, very similar to LaFeAsO, which is the parent compound of the iron arsenide superconductors. BaFe$_2$As$_2$ is a poor Pauli-paramagnetic metal and undergoes a structural and magnetic phase transition at 140 K, accompanied by strong anomalies in the specific heat, electrical resistance, and magnetic susceptibility. In the course of this transition, the space-group symmetry changes from tetragonal ($I4/mmm$) to orthorhombic ($Fmmm$). ^{57}Fe Mössbauer spectroscopy experiments show a single signal at room temperature and full hyperfine field splitting below the phase-transition temperature (5.2 T at 77 K). Our results suggest that BaFe$_2$As$_2$ can serve as a parent compound for oxygen-free iron arsenide superconductors.

The recent discovery of superconductivity in doped iron arsenide oxides[1] has heralded a new era in superconductivity research.[2] After the first report on LaFeAs(O$_{1-x}$F$_x$) with a critical temperature T_C of 26 K, even higher transition temperatures up to 55 K in fluoride doped SmFeAs(O$_{1-x}$F$_x$) followed quickly.[3] It is meanwhile accepted that these materials represent the second class of high-T_C superconductors after the discovery of the cuprates more than 20 years ago.[4] The parent compound LaFeAsO crystallizes in the tetragonal ZrCuSiAs-type structure (space group $P4/nmm$).[5] Layers of edge-sharing OLa$_{4/4}$ tetrahedra alternate with layers of FeAs$_{4/4}$ tetrahedra along the c axis, as shown on the left-hand side in Fig. 1. This two-dimensional character of LaFeAsO involves different types of chemical bonding, which is strongly ionic in the LaO layers and rather covalent in the FeAs layers, respectively. From this purely ionic perception, we can assume a charge transfer according to $(\text{LaO})^{\delta+}(\text{FeAs})^{\delta-}$.

It is currently believed that the superconductivity in doped LaFeAsO is like in the cuprates, not of s-wave-type, but intimately connected with magnetic fluctuations and a spin-density-wave (SDW) anomaly within the FeAs layers.[6,7] Undoped LaFeAsO undergoes a SDW-driven structural phase transition around 150 K, associated with a reduction of the lattice symmetry from tetragonal to orthorhombic[8] and

FIG. 1. Crystal structures of LaFeAsO (left, ZrCuSiAs type) and BaFe$_2$As$_2$ (right, ThCr$_2$Si$_2$ type).

anomalies in the specific heat, electrical resistance, and the magnetic susceptibility. Antiferromagnetic ordering of the magnetic moments ($0.36\mu_B$/Fe) was found below T_N = 134 K by neutron scattering.[9] Electron doping with fluoride or oxygen deficiency, as well as hole doping with strontium, suppresses the phase transition and the tetragonal phase becomes superconducting at T_C = 25–41 K.[1,10,11] Hence, there is a strong evidence that superconductivity in LaFeAsO emerges primarily from specific structural and electronic conditions of the (FeAs)$^{\delta-}$ layers.

Another well-known structure type provides very similar conditions. The ternary iron arsenide BaFe$_2$As$_2$, with the tetragonal ThCr$_2$Si$_2$-type structure (space group $I4/mmm$),[12] contains practically identical layers of edge-sharing FeAs$_{4/4}$ tetrahedra, but they are separated by barium atoms instead of LaO sheets. Figure 1 shows both structures in comparison. In the very large family of ThCr$_2$Si$_2$-type compounds, superconductivity occurs scarcely and only at temperatures below 5 K.[13] Examples are LaIr$_2$Ge$_2$, LaRu$_2$P$_2$, YIr$_{2-x}$Si$_{2+x}$, and BaNi$_2$P$_2$.[14–17] In contrast to this, the related borocarbides are superconductors with higher T_C's up to 26 K in YPd$_2$B$_2$C.[18] We suggested earlier that superconductivity in ThCr$_2$Si$_2$-type compounds may be associated with direct interactions between the transition-metal atoms, which can lead to structural instabilities.[19]

Regarding the previously described structural and electronic properties of LaFeAsO, we believe that among the ThCr$_2$Si$_2$-type compounds, BaFe$_2$As$_2$ is a very promising candidate for superconductivity for both structural and electronic reasons. In addition to the closely related geometry, the electron counts of the FeAs layers in BaFe$_2$As$_2$ and LaFeAsO are identical because in both cases, one electron is transferred to FeAs according to Ba$_{0.5}^{2+}$(FeAs)$^-$ and (LaO)$^+$(FeAs)$^-$, respectively. Apart from the indeterminate magnetic data,[20] no physical properties of BaFe$_2$As$_2$ are known so far. In this Rapid Communication, we report on a structural and magnetic phase transition at 140 K, specific heat, resistivity, and magnetic measurements, as well as ^{57}Fe Mössbauer spectroscopy of BaFe$_2$As$_2$. We can show that the
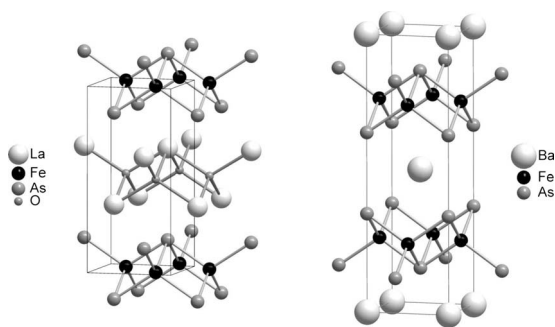
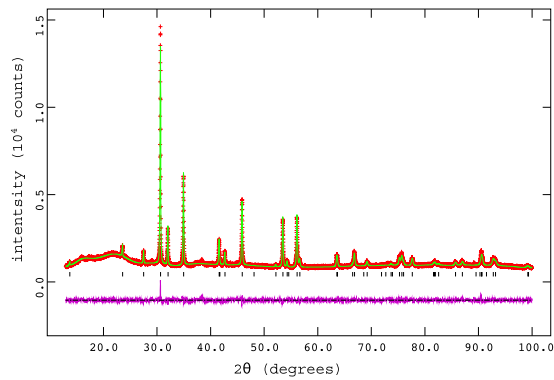FIG. 2. (Color online) X-ray powder pattern (+) and Rietveld fit (−) of $BaFe_2As_2$ at 297 K (space group $I4/mmm$).

FIG. 4. (Color online) X-ray powder pattern (+) and Rietveld fit (−) of $BaFe_2As_2$ at 20 K (space group $Fmmm$).

structural, electronic, and magnetic properties of $BaFe_2As_2$ and LaFeAsO are remarkably similar, which renders $BaFe_2As_2$ as a potential parent compound for oxygen-free superconductors based on the $ThCr_2Si_2$-type structure.

$BaFe_2As_2$ was synthesized by heating a mixture of distilled barium metal, H_2-reduced iron powder, and sublimed arsenic at a ratio of $1.05:2:2$ in an alumina crucible, which was sealed in a silica tube under an atmosphere of purified argon. The mixture was heated to 1123 K at a rate of 50 K/h, it was kept at this temperature for 10 h and cooled down to room temperature. The reaction product was homogenized in an agate mortar and annealed at 1173 K for 25 h. After cooling, the sample was homogenized again, pressed into a pellet ($\varnothing=5$ mm, 1 mm thick), and sintered at 973 K. The obtained black crystalline powder of $BaFe_2As_2$ is stable in air. Phase purity was checked by x-ray powder diffraction using a Huber G670 Guinier imaging plate diffractometer (Cu-$K\alpha_1$ radiation, Ge-111 monochromator), equipped with a closed-cycle He-cryostat. Rietveld refinements of $BaFe_2As_2$ were performed with the GSAS package[21] using Thompson-Cox-Hastings functions with asymmetry corrections as reflection profiles.[22] Figure 2 shows the pattern of $BaFe_2As_2$, which could be completely fitted with a single phase. Impurities are, if at all, less than 1%.

In order to check for a phase transition at about 150 K, as known from LaFeAsO, we measured the specific heat between 3 and 200 K by a relaxation-time method in a physical properties measurement system (PPMS, Quantum Design, Inc.). As can be clearly seen from Fig. 3, we find a pro-
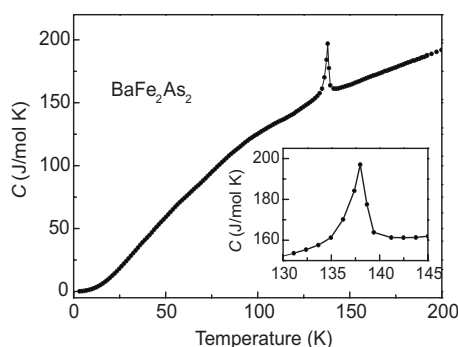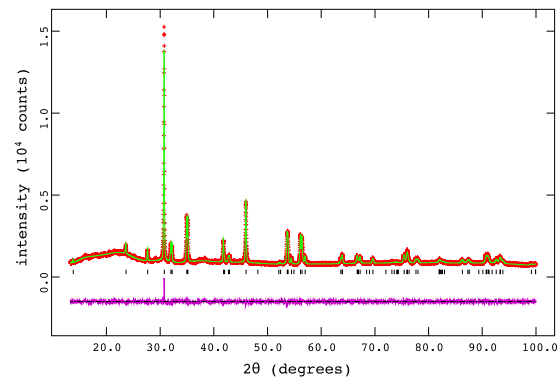
nounced anomaly of $C_p(T)$ at ≈ 140 K. The characteristic λ-like shape of the peak points to a second-order transition, as is typical for magnetic ordering or a displacive structural change. From the inflection point of the λ anomaly, we extracted the transition temperature of 139.9 ± 0.5 K. In the low-temperature region, the specific heat is of the form $C_p = \gamma T + \beta T^3$. The Debye temperature can be estimated from the equation $\beta = (12\pi^4 nk_B)/(5\Theta_D^3)$, where n is the number of atoms per formula unit. From a C_p/T vs T^2 plot between 3.1 and 14 K, we determined $\gamma = 16(2)$ mJ K^{-2} mol^{-1}, $\beta = 2.0(5)$ mJ K^{-4} mol^{-1}, and $\Theta_D = 134(1)$ K.

Subsequently we have recorded x-ray powder patterns of $BaFe_2As_2$ between 297 and 20 K. Several reflections broaden below 140 K and clearly split with further decreasing temperature. The patterns below 136 K were indexed with an orthorhombic F-centered unit cell ($a_{ortho} = \sqrt{2} \cdot a_{tetra} - \delta$; $b_{ortho} = \sqrt{2} \cdot b_{tetra} + \delta$; $c_{ortho} \approx c_{tetra}$; $\delta \approx 5$ pm). The low-temperature data could be refined in the space group $Fmmm$. Figure 4 shows the Rietveld fit of the data at 20 K. The continuous transition of the pattern between 150 and 40 K, as well as the variation of the lattice parameters, is depicted in Fig. 5. The space group $Fmmm$ is a subgroup of $I4/mmm$, thus, a second-order phase transition is in agreement with our data. In terms of group theory, this transition is *translationengleich* with index two ($I4/mmm \xrightarrow{t2} Fmmm$). Crystallographic data are summarized in Table I. The main effect of the phase transition appears in the Fe-Fe distances,

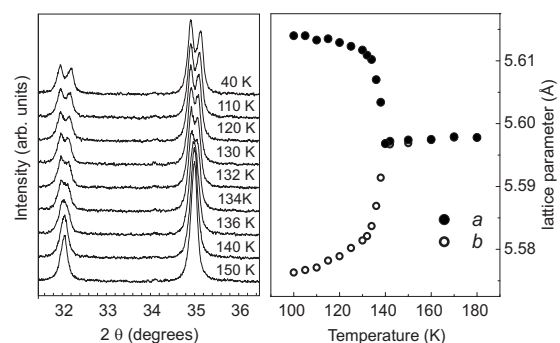

FIG. 3. Specific heat of $BaFe_2As_2$ vs temperature.

FIG. 5. Splitting of the 110 and 112 reflections and variation of the lattice parameters with temperature. Values for the tetragonal phase above 140 K are multiplied by $\sqrt{2}$ for comparability.

TABLE I. Crystallographic data of $BaFe_2As_2$.

Temperature (K)	297	20
Space group	$I4/mmm$	$Fmmm$
a (pm)	396.25(1)	561.46(1)
b (pm)	$=a$	557.42(1)
c (pm)	1301.68(3)	1294.53(3)
V (nm^3)	0.20438(1)	0.40514(2)
Z	2	4
Data points	8700	8675
Reflections	50	74
Atomic parameters	4	4
Profile parameters	4	4
d range	0.979–6.508	0.981–6.473
R_P, wR_P	0.0273, 0.0358	0.0283, 0.0365
$R(F^2)$, χ^2	0.0522, 1.431	0.0576, 1.392
Atomic parameters		
Ba	$2a$ (0,0,0)	$2a$ (0,0,0)
	$U_{iso}=95(5)$	$U_{iso}=69(5)$
Fe	$4d$ $(\frac{1}{2},0,\frac{1}{4})$	$8f$ $(\frac{1}{4},\frac{1}{4},\frac{1}{4})$
	$U_{iso}=57(6)$	$U_{iso}=64(4)$
As	$4e$ (0,0,z)	$8i$ (0,0,z)
	$z=0.3545(1)$	$z=0.3538(1)$
	$U_{iso}=99(5)$	$U_{iso}=65(5)$
Bond lengths (pm)		
Ba–As	338.2(1)×8	336.9(1)×4,
		338.5(1)×4
Fe–As	240.3(1)×4	239.2(1)×4
Fe–Fe	280.2(1)×4	280.7(1)×2,
		278.7(1)×2
Bond angles (deg)		
As-Fe-As	111.1(1)×2	111.6(1)×2
	108.7(1)×4	108.7(1)×2,
		108.1(1)×2

where four equal bonds of 280.2 pm length split into two pairs of 280.8 and 278.7 pm length. This supports the idea that the Fe-Fe interactions are strongly correlated with the SDW anomaly and may play a certain role for the properties of $BaFe_2As_2$.

So far, our results clearly prove a structural distortion in $BaFe_2As_2$. The nature of this effect is completely analogous to that in LaFeAsO, where a transition from the tetragonal space group $P4/nmm$ to the orthorhombic space group $Cmme$ occurs.[8] As mentioned above, the transition of LaFeAsO is driven by SDW instability within the iron layers and, therefore, causes anomalies in the electrical resistivity and magnetic susceptibility. We have measured these properties of $BaFe_2As_2$ and again found very similar behavior. The temperature dependency of the dc electrical resistance is depicted in Fig. 6. $BaFe_2As_2$ is a poor metal with a relatively high resistance around 1 mΩ cm at room temperature, which decreases only slightly on cooling. At 140 K, the resistance drops abruptly at first but then decreases monotonically to 0.2 mΩ cm at 10 K. This behavior corresponds to
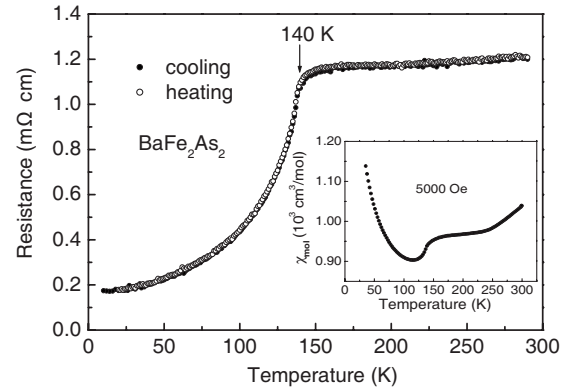

FIG. 6. dc electrical resistance of $BaFe_2As_2$ ($I=100$ μA). Inset. Magnetic susceptibility measured at 0.5 T.

undoped LaFeAsO, where the resistance is of the same magnitude at room temperature and drops in a similar fashion.[6]

Finally we have investigated the general magnetic properties and the specific behavior at the phase transition. The magnetic susceptibility was measured with a superconducting quantum interference device (SQUID) magnetometer (MPMS-XL5, Quantum Design, Inc.) at 0.5 T. $BaFe_2As_2$ shows a weak and only slightly temperature-dependent paramagnetism, as is typical for a Pauli-paramagnetic metal. Below 140 K, χ drops at first but it increases again below 100 K. The latter fact may be attributed to traces of ferromagnetic impurities, which are not detectable by the x-ray powder method.

A ^{57}Co/Rh source was available for ^{57}Fe Mössbauer spectroscopy investigations. The $BaFe_2As_2$ sample was placed in a thin-walled PVC container at a thickness of about 4 mg Fe/cm^2. The measurements were performed in the usual transmission geometry at 298, 77, and 4.2 K, and the source was kept at room temperature. ^{57}Fe Mössbauer spectra of $BaFe_2As_2$ at 298, 77, and 4.2 K are shown in Fig. 7, together with the transmission integral fits. The corresponding fitting parameters are listed in Table II. At room temperature, we observed a single signal at an isomer shift of δ =0.31(1) mm· s^{-1}. Although the iron atoms have a noncubic coordination by arsenic, there was no need to consider quadrupole splitting in the fits. The observed isomer shift is slightly smaller than in $SmFeAsO_{0.85}$[23] and LaFeAsO.[24,25] At 77 K, well below the transition temperature, we observe a significant hyperfine field splitting with a hyperfine field value of 5.23(1) T, which is even slightly larger than the hyperfine field observed for LaFeAsO (4.86 T).[25] A very small quadrupole splitting parameter of −0.03(1) mm/s was included in the fits. This parameter accounts for the small tetragonal-to-orthorhombic structural distortion. A similar value has been observed for the SDW system LaFeAsO below the transition temperature.[24] The quadrupole splitting parameter slightly increases to −0.04(1) mm/s at 4.2 K (Table II). The hyperfine field at the iron nuclei is 5.47(1) T and the corresponding magnetic moment was estimated as 0.4μ_B per iron atom.

In summary, we have shown that the properties of the ternary arsenide $BaFe_2As_2$ with the $ThCr_2Si_2$-type structure are remarkably similar to LaFeAsO, which is the parent com-
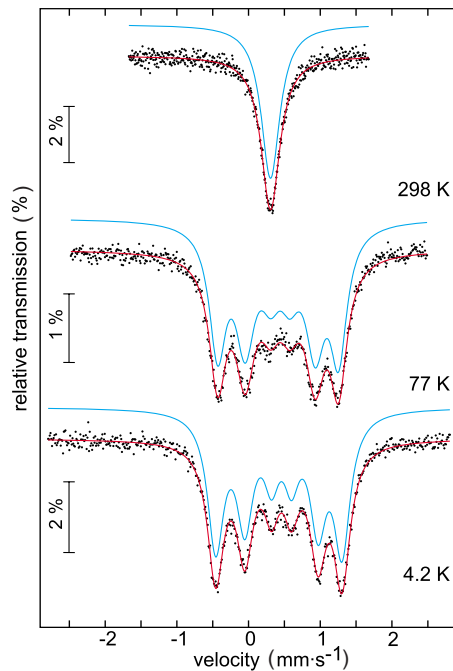
FIG. 7. (Color online) ^{57}Fe Mössbauer spectra of BaFe$_2$As$_2$ with transmission integral fits.

TABLE II. Fitting parameters of ^{57}Fe Mössbauer spectroscopy measurements with BaFe$_2$As$_2$.

T (K)	δ (mm·s^{-1})	Γ (mm·s^{-1})	ΔE_Q (mm·s^{-1})	B_{hf} (T)
295	0.31(1)	0.32(1)		
77	0.43(1)	0.33(2)	−0.03(1)	5.23(1)
4.2	0.44(1)	0.25(1)	−0.04(1)	5.47(1)

ting below 140 K, which also hints at antiferromagnetic ordering. Consequently, BaFe$_2$As$_2$ exhibits the same SDW anomaly at 140 K as LaFeAsO at 150 K. Since this SDW instability is actually believed to be an important prerequisite for high-T_C superconductivity in iron arsenides, our results strongly suggest that BaFe$_2$As$_2$ can serve as a parent compound for another oxygen-free class of iron arsenide superconductors with ThCr$_2$Si$_2$-type structure. All the signs are that the superconductivity in BaFe$_2$As$_2$ can be induced either by electron or hole doping. If this is the case, it would conclusively prove that superconductivity originates only from the iron arsenide layers, regardless of the separating sheets. On the other hand, superconductivity in doped BaFe$_2$As$_2$ would open new avenues to further high-T_C materials in the large family of ThCr$_2$Si$_2$-type compounds.

*johrendt@lmu.de

[1] Y. Kamihara, T. Watanabe, M. Hirano, and H. Hosono, J. Am. Chem. Soc. **130**, 3296 (2008).

[2] D. Johrendt and R. Pöttgen, Angew. Chem., Int. Ed. **47**, 4782 (2008).

[3] Z.-A. Ren *et al.*, Chin. Phys. Lett. **25**, 2215 (2008).

[4] J. G. Bednorz and K. A. Müller, Z. Phys. B: Condens. Matter **64**, 189 (1986).

[5] V. Johnson and W. Jeitschko, J. Solid State Chem. **11**, 161 (1974).

[6] J. Dong, H. J. Zhang, G. Xu, Z. Li, G. Li, W. Z. Hu, D. Wu, G. F. Chen, X. Dai, J. L. Luo, Z. Fang, and N. Wang, Europhys. Lett. **83**, 27006 (2008).

[7] G. F. Chen, Z. Li, D. Wu, G. Li, W. Z. Hu, J. Dong, P. Zheng, J. L. Luo, and N. L. Wang, Phys. Rev. Lett. **100**, 247002 (2008).

[8] T. Nomura, S. W. Kim, Y. Kamihara, M. Hirano, P. V. Sushko, K. Kato, M. Takata, A. L. Shluger, and H. Hosono, arXiv:0804.3569 (unpublished).

[9] C. de la Cruz *et al.*, Nature (London) **453**, 899 (2008).

[10] W. Lu, X.-L. Shen, J. Yang, Z.-C. Li, W. Yi, Z.-A. Ren, X.-L. Dong, G.-C. Che, L.-L. Sun, F. Zhou, and Z. Zhao, arXiv:0804.3725 (unpublished).

[11] H.-H. Wen, G. Mu, L. Fang, H. Yang, and X. Zhu, Europhys. Lett. **82**, 17009 (2008).

[12] M. Pfisterer and G. Nagorsen, Z. Naturforsch. B **35**, 703 (1980).

[13] R. N. Shelton, H. F. Braun, and E. Musick, Solid State Commun. **52**, 797 (1984).

[14] M. Francois, G. Venturini, J. F. Mareche, B. Malaman, and B. Roques, J. Less-Common Met. **113**, 231 (1985).

[15] W. Jeitschko, R. Glaum, and L. Boonk, J. Solid State Chem. **69**, 93 (1987).

[16] M. Hirjak, P. Lejay, B. Chevalier, J. Etourneau, and P. Hagenmuller, J. Less-Common Met. **105**, 139 (1985).

[17] T. Mine, H. Yanagi, T. Kamiya, Y. Kamihara, M. Hirano, and H. Hosono, Solid State Commun. **147**, 111 (2008).

[18] R. J. Cava *et al.*, Nature (London) **367**, 252 (1994).

[19] D. Johrendt, C. Felser, O. Jepsen, O. K. Andersen, A. Mewis, and J. Rouxel, J. Solid State Chem. **130**, 254 (1997).

[20] M. Pfisterer and G. Nagorsen, Z. Naturforsch. B **38**, 811 (1983).

[21] A. C. Larson and R. B. V. Dreele, *General Structure Analysis System*, Los Alamos National Laboratory Report LAUR 86 (2004).

[22] L. W. Finger, D. E. Cox, and A. P. Jephcoat, J. Appl. Crystallogr. **27**, 79 (1992).

[23] I. Felner, I. Nowik, M. Tsindlekht, Z.-A. Ren, X.-L. Shen, G.-C. Che, and Z.-X. Zhao, arXiv:0805.2794 (unpublished).

[24] S. Kitao, Y. Kobayashi, S. Higashitanguchi, M. Saito, Y. Kamihara, M. Hirano, T. Mitsiu, H. Hosono, and M. Seto, arXiv:0805.0041 (unpublished).

[25] H.-H. Klauss, H. Luetkens, R. Klingeler, C. Hess, F. Litterst, M. Kraken, M. M. Korshunov, I. Eremin, S.-L. Drechsler, R. Khasanov, A. Amato, J. Hamannborreo, N. Leps, A. Kondrat, G. Behr, J. Werner, and B. Buchner, arXiv:0805.0264 (unpublished).